Dynamical Preparation of Quantum Spin Liquids in Rydberg Atom Arrays

Giuliano Giudici,[1,2,3,4] Mikhail D. Lukin,[5] and Hannes Pichler[1,2]
[1]Institute for Theoretical Physics, University of Innsbruck, Innsbruck A-6020, Austria
[2]Institute for Quantum Optics and Quantum Information, Austrian Academy of Sciences, Innsbruck A-6020, Austria
[3]Munich Center for Quantum Science and Technology (MCQST), Schellingstraße 4, D-80799 München, Germany
[4]Arnold Sommerfeld Center for Theoretical Physics, University of Munich, Theresienstraße 37, 80333 München, Germany
[5]Department of Physics, Harvard University, Cambridge, Massachusetts 02138, USA

(Received 20 January 2022; accepted 3 August 2022; published 22 August 2022)

We theoretically analyze recent experiments [Semeghini *et al.*, Science **374**, 1242 (2021)] demonstrating the onset of a topological spin liquid using a programmable quantum simulator based on Rydberg atom arrays. In the experiment, robust signatures of topological order emerge in out-of-equilibrium states that are prepared using a quasiadiabatic state preparation protocol. We show theoretically that the state preparation protocol can be optimized to target the fixed point of the topological phase—the resonating valence bond state of hard dimers—in a time that scales linearly with the number of atoms. Moreover, we provide a two-parameter variational manifold of tensor network states that accurately describe the many-body dynamics of the preparation process. Using this approach we analyze the nature of the nonequilibrium state, establishing the emergence of topological order.

DOI: 10.1103/PhysRevLett.129.090401

Introduction.—Quantum spin liquids (QSLs) arise from the competition between classical frustration and quantum fluctuations [1–6]. They are paradigmatic examples of topological quantum matter [5,6], characterized by long-range entanglement [7], hidden nonlocal order [5], and exotic excitations [8]. Experimental preparation and control of topological matter is of central importance not only for understanding these many-body quantum phenomena but also for realizing novel approaches to fault-tolerant topological quantum computation [7,9]. Recently, the onset of a topological spin liquid has been observed in a quantum simulator based on Rydberg atom arrays [10]. The key idea is to exploit the Rydberg blockade mechanism [11–15] to realize a dimer model, where spin liquid states are known to emerge as equilibrium states at zero temperature [16–18]. These states share many similarities with a resonating valence bond (RVB) state [19] of hard dimers, where the role of a dimer is played by an excited Rydberg state on the medial lattice of a kagome lattice [Fig. 1(a)]. While the RVB state is an equal weight superposition of all the maximal dimer coverings of the kagome lattice, the Rydberg array can accommodate defects in the form of uncovered kagome vertices. Theoretical analysis showed that the presence of a topological phase depends delicately on the precise details of the Rydberg interactions and atomic positions [11]. Remarkably, experiments showed that robust signatures of quantum spin liquids appear using quasiadiabatic detuning sweeps employed in Ref. [10], even in regimes where quantum spin liquids are not expected to be stable as the ground state. Understanding the dynamical preparation process, the robustness of the emerging state, the role of the defects, and the extent to which they can be reduced is crucial for determining the physical properties of the nonequilibrium state as well as its potential utility for topological quantum information processing.

In this Letter, we investigate the state produced through the quasiadiabatic sweep by simulating the quantum dynamics via exact and variational methods. We show that the defect-free RVB state can be prepared with high fidelity in a time that scales linearly with the number of atoms. To understand the nature of the defects generated during the state preparation protocol utilized in the experiments [10], we introduce a novel tensor network (TN) ansatz. We demonstrate that it accurately describes the entire many-body dynamics of the preparation process, and we analyze the resulting phase diagram via TN techniques. The latter allows us to study the properties of the nonequilibrium state on system sizes comparable to experiments [10]. By computing several witnesses, including nonlocal order parameters [20,21] and topological entanglement entropy [22,23], we establish the presence of an extended region in parameter space that is adiabatically connected to the RVB state and hosts topological order.

Model Hamiltonian and RVB state preparation.—The Rydberg atom quantum simulator of Ref. [10] consists of neutral atoms optically trapped in fixed positions on the links of a kagome lattice. Optical transitions between the ground state $|g\rangle$ and the excited Rydberg state $|r\rangle$ of each atom are controlled via a two-photon process with Rabi frequency Ω and detuning Δ. Excited Rydberg states interact through van der Waals potential. The effective Hamiltonian is [24,25]

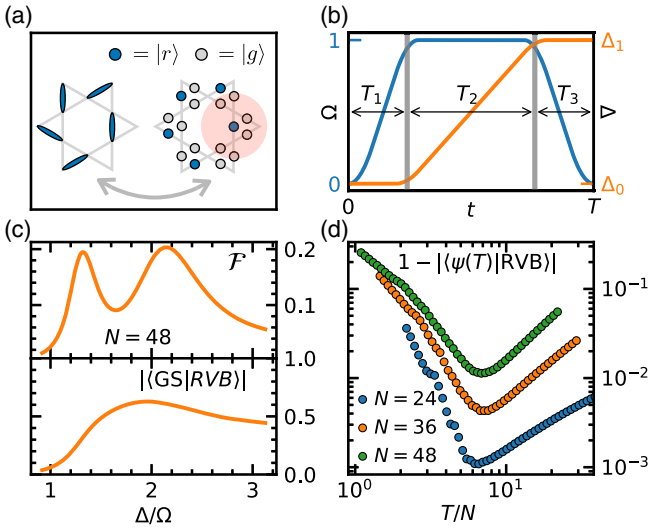

FIG. 1. (a) Mapping between a dimer model on the kagome lattice and the Rydberg atoms system on the ruby lattice. When $R_b \gtrsim 2a$ (shaded red circle) the Rydberg constraint is equivalent to the dimer constraint. (b) Schematic representation of the adiabatic state preparation protocol. The vertical gray lines separate the three stages of the preparation process: ramp-up of Ω and Δ, and ramp-down of Ω. (c) Top: ground state fidelity susceptibility $\mathcal{F} = (1 - |\langle \mathrm{GS}(\lambda)|\mathrm{GS}(\lambda + d\lambda)\rangle|)/d\lambda$ with $\lambda = \Omega/\Delta$ and $d\lambda = 0.0025$. Bottom: RVB overlap with the ground state of the Hamiltonian Eq. (1). (d) Overlap between the dynamically prepared state and the RVB state as a function of the total sweep time T rescaled with the number of atoms N, for $\Delta_0 = -5$, $\Delta_1 = 1.5$, $T_1 = T_3 = 0.1T$, and $T_2 = 0.8T$.

$$H = \frac{\Omega}{2}\sum_i \sigma_i^x - \Delta\sum_i n_i + V\sum_{i>j}\frac{n_i n_j}{|i-j|^6}, \qquad (1)$$

where $\sigma_i^x = |g\rangle_i\langle r| + |r\rangle_i\langle g|$ and $n_i = |r\rangle_i\langle r|$. The parameter V is tuned by varying the lattice spacing, and its magnitude determines the blockade radius $R_b = (V/\Omega)^{1/6}$. The interactions effectively suppress simultaneous occupancy of excited Rydberg states at distance $r \leq R_b$. Numerical calculations are performed enforcing this constraint exactly on periodic clusters at $R_b = 2a$, where a is the minimum distance between the atoms. Moreover, we neglect longer-range tails of the interactions at $r > R_b$ [Fig. 1(a)]. The effect of the tails and of a relaxed blockade constraint is described in the final part of this Letter. The phase diagram of the simplified model hosts three phases: trivially disordered, topologically ordered, and trivially ordered as Δ increases [11]. These three phases can be identified from the exact diagonalization calculations plotted in Fig. 1(c). The upper panel shows two clear peaks in the ground state fidelity susceptibility $\mathcal{F} = (1 - |\langle \mathrm{GS}(\lambda)|\mathrm{GS}(\lambda + d\lambda)\rangle|)/d\lambda$ that signal an intermediate phase, characterized by high overlap ($\simeq$0.7 for $N = 48$ atoms) with the RVB state.

We first focus on state preparation protocols depicted in Fig. 1(b). The initial state is the vacuum, where all the atoms are in their ground states. The driving field is turned on at fixed detuning Δ_0 and Ω increases until it reaches its maximum value (which sets our unit of energy and time). The detuning is then increased from Δ_0 to Δ_1. Finally, Ω is switched off at fixed detuning Δ_1. The durations of the three stages of the sweep are T_1, T_2, T_3, respectively, and the total time is T. These parameters can be tuned at will, and we choose $T_1 = T_3 = 0.1T$, $T_2 = 0.8T$, $\Delta_0 = -5$, and $\Delta_1 = 1.5$ in units of the maximum Rabi frequency. The final result moderately depends on the parameter Δ_1, while it is mildly affected by the others [26]. Figure 1(d) shows the overlap of the final state with the defect-free RVB state as a function of the total time T. The large and small T regimes are characterized by small overlap with the RVB state. In the former, one recovers the adiabatic limit, where the final state is a valence bond solid (VBS), i.e., the ground state at large detuning [11]. In the latter, the high sweep rate creates a high density of defects on top of the maximal density subspace. Remarkably, at intermediate T the prepared state reaches 0.99 fidelity with the RVB state for $N = 48$ atoms. The maximal overlap with the RVB state is obtained at a time T^* that scales linearly with system size N, as it is evident from Fig. 1(d), where the overlap is plotted as a function of T/N. We note that RVB fidelities of the dynamically prepared state exceed the ground state ones by almost 2 orders of magnitude [Figs. 1(c) and 1(d)].

Ansatz for the preparation dynamics.—We now expand our focus beyond the analysis of the final state at the end of the sweep, and aim at developing an understanding of the dynamics of the system during the state preparation protocol. We are particularly interested in regimes where the dynamics is not adiabatic and the resulting density of monomers is not vanishingly small. For this we find it convenient to slightly modify the state preparation protocol, to the one depicted in the inset of Fig. 2(a): after initially switching on Ω, the detuning is linearly increased until the end of the process, i.e., we set T_3 to zero [cf. Fig. 1(b)]. We focus on the state generated at intermediate values of the detuning during this preparation protocol. Similar to the previous section, we will use the total sweep time T as a parameter to interpolate from a sudden quench to a perfectly adiabatic dynamics where the system is in the instantaneous ground state. To describe the state of the system during this dynamics we introduce the following variational ansatz:

$$|\phi(z_1, z_2)\rangle = \mathcal{N}\mathcal{P}\left[\bigotimes_{i=1}^{N}(1 + z_2\sigma_i^+)(1 + z_1\sigma_i^-)\right]|\phi_0\rangle, \qquad (2)$$

where $z_1, z_2 \in \mathbb{C}$. Here, $|\phi_0\rangle$ is the equal-weight superposition of configurations corresponding to defect-free dimer covering, i.e. the RVB state, and $\mathcal{P}$ is the projector on the blockade-constraint satisfying sector of the Hilbert space, $\sigma_i^- = |g\rangle_i\langle r|$, $\sigma_i^+ = |r\rangle_i\langle g|$ and $\mathcal{N}$ is a normalization

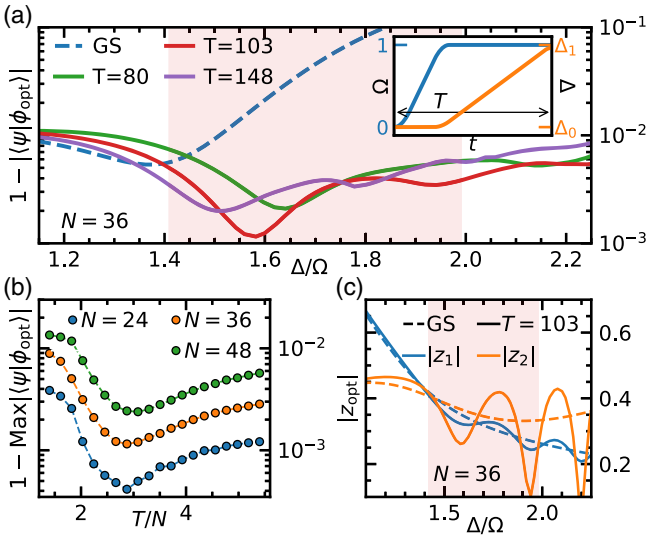

FIG. 2. (a) Overlap between the dynamically prepared state during the sweep (depicted in the inset) and the ansatz Eq. (2), optimized over the variational parameters z_1, z_2 for various sweep times T, for a periodic cluster of $N = 36$ atoms. The dashed line is the optimized overlap with the instantaneous ground state ($T = \infty$). The shaded red region delimits the topological phase in the ground state. (b) Maximal overlap obtained during the sweep when $1 \lesssim \Delta/\Omega \lesssim 2$, for different N, as a function of the total sweep time rescaled by N [29]. (c) Optimal absolute values for the variational parameters z_1, z_2 in the ansatz state during a semiadiabatic sweep with $T = 103$ (solid line) and on the ground state (dashed line) for $N = 36$.

constant. We allow the two variational parameters z_1, z_2 to be complex to capture relative phases between fixed density subspaces. To understand this manifold of states it is instructive to consider the limiting cases. In one limit, where $z_1 = \infty$ and $z_2 = 0$, the state reduces to the trivial vacuum state, i.e., the initial state of the experimental state preparation protocol. In another limit, when $z_1 = z_2 = 0$, the state is simply the RVB state. In the vicinity of this point, the parameters z_1, z_2 control the properties of defects on top of the RVB state. These defects are monomers, i.e., vertices of the kagome lattice that are not covered by a dimer. Specifically, a finite value of the parameter z_1, results in the creation of nearest-neighbor monomer pairs that are created by removing a dimer from a dimer covering. The value of z_1 controls the density of such pairs. A finite value of z_2 effectively allows these monomer pairs to separate, introducing pairs with larger intrapair distances. Finally, in the limit when $z_1 = \infty$, all monomers are uncorrelated and their density is set by z_2. This last limiting case has been previously employed in variational studies of ground states for Rydberg atom arrays on the square lattice, and its norm maps to a classical partition function with local weights [28]. An important feature of the state $|\phi(z_1, z_2)\rangle$ is that it is a TN state of bond dimension 4 for all z_1, z_2. This follows from the observations that the RVB state is a TN state of bond dimension 2, and $\mathcal{P}$ is a TN operator with the same bond dimension. We note that expectation values for this state can be computed exactly by the contraction of a tensor network of bond dimension 8 [26].

We demonstrate the effectiveness of the ansatz Eq. (2) in Fig. 2(a), where we plot the optimized overlap with the dynamically evolving state for various total sweep times T (solid lines) in a periodic cluster of $N = 36$ atoms [26]. The dashed line denotes the optimized overlap with the instantaneous ground state, which corresponds to a fully adiabatic sweep with $T = \infty$. The shaded red region indicates the topological phase in the ground state phase diagram. Our ansatz best describes the ground state in a neighborhood of the transition point between topological and disordered phases, at $\Delta/\Omega \simeq 1.4$. This is expected, as the ansatz Eq. (2) does not break any lattice symmetry, and as such does not include the VBS ground state at large detuning, causing a suppression of the overlap as the VBS phase is approached. During the preparation dynamics, the highest overlaps with the variational state are obtained for intermediate T. Figure 2(b) shows that the fidelity slowly decreases with the number of atoms, but remains impressively large for all the system sizes considered (> 0.99 for $N = 48$ atoms). Similar to what we observed for the pure-RVB preparation protocol, the total sweep time for which maximal fidelities are reached increases linearly with N. In Fig. 2(c) we plot the magnitude of the optimal values for the two variational parameters, for the fully adiabatic sweep (dashed line) and the optimal sweep rate for $N = 36$.

These optimal values are to be located in the state phase diagram reported in Fig. 3(a) that shows the derivative of the density of Rydberg excitations computed via TN methods on an infinite cylinder with circumference of length 12 links of the kagome lattice ($L = 6$ tensors) [26]. The presence of a peak in the derivative points at two distinct phases: an RVB-like phase and a trivial phase when z_1, z_2 are small and large, respectively. A closer inspection of the scaling of the peak with the length of the circumference [26] confirms a continuous phase transition separating a topological phase, connected to the RVB state, and a trivial phase connected to the vacuum. We demonstrate that the latter has topological order by showing in Fig. 3(b) the topological entanglement entropy γ of the state Eq. (2) on a periodic cluster of $N = 48$ sites, obtained from $\gamma = S_{AB} + S_{BC} + S_{AC} - S_A - S_B - S_C - S_{ABC}$ [22,23], where S_X is the entanglement entropy of the subsystem X, see Fig. 3(c). A value close to ln 2 signals $\mathbb{Z}_2$ topological order in the region conntected to the RVB point. To further corroborate the topological nature of the high-density phase we compute the Bricmont-Frölich-Fredenhagen-Marcu (BFFM) [20,21] order parameters, as defined in Ref. [11]. These order parameters are defined on a loop of length ℓ and, in a topologically ordered phase, they vanish when $\ell \to \infty$. In Fig. 3(c) we plot the diagonal and off-diagonal BFFM order parameters obtained from hexagonal loops of perimeter $\ell = 18$ links of the kagome

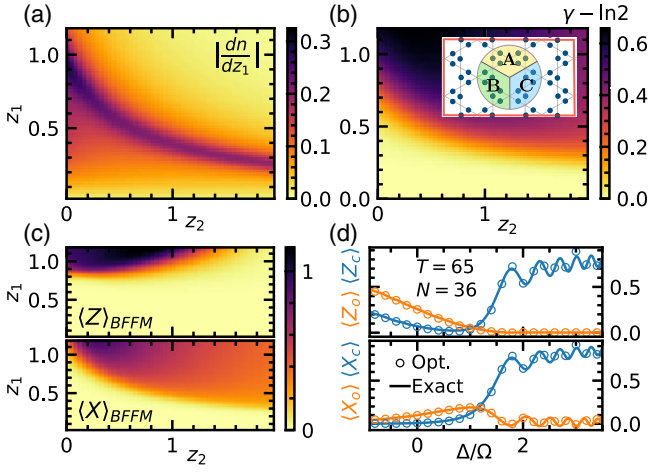

FIG. 3. (a) Derivative of the density with respect to the parameter z_1, computed from the TN representation of the ansatz Eq. (2) on an infinite cylinder of circumference $L = 6$ tensors. (b) Topological entanglement entropy γ of the ansatz computed on the finite cluster of $N = 48$ sites depicted in the inset. (c) Diagonal and off-diagonal BFFM order parameters on the infinite cylinder of circumference $L = 6$. (d) Expectation values of open and closed string operators obtained during the dynamical preparation (solid lines) and from the optimized ansatz (empty markers) for $N = 36$ and $T = 65$.

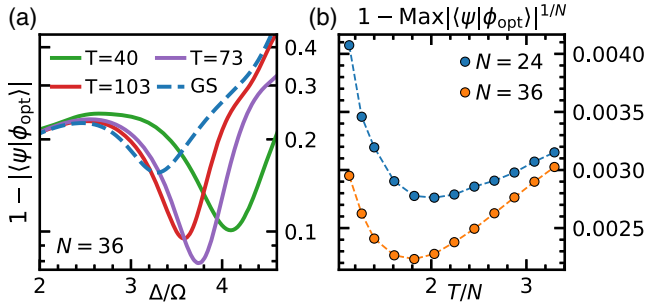

FIG. 4. (a) Optimized overlap between the ansatz Eq. (2) (without projector $\mathcal{P}$) and the state prepared through the sweep depicted in the inset of Fig. 2(a) for different total sweep times T. The dynamics is generated by the full Rydberg Hamiltonian Eq. (1) with $R_b = 2.4a$. (b) Maximal fidelity per site obtained during the sweep as a function of the total sweep time T rescaled by the number of atoms N.

lattice on an infinite cylinder with $L = 6$ [26]. The region where both these observables are small coincides with the conjectured topological phase. We checked that, in this region, they vanish exponentially with increasing loop length [26]. In Fig. 3(c) we compare the building blocks of the BFFM order parameters, namely expectation values of string operators Z_o (X_o) and Z_c (X_c) on open and closed strings, computed during the preparation process and obtained from the optimized ansatz Eq. (2) for a loop of length $\ell = 6$ [26]. We observe good agreements even for short preparation times.

Effect of long-range interactions.—To study the state preparation dynamics generated by the full Rydberg Hamiltonian Eq. (1) we include long-range tails of the Rydberg interaction and set $R_b = 2.4a$. The maximal interaction distance between two excited Rydberg states is $|i - j| = \sqrt{13}a$. Moreover, we relax the radius of the hard constraint of Fig. 1(a) to one length unit, such that each triangle has at most one dimer. While the relaxation of the constraint notably improves the overlap with the RVB state [26], the inclusion of long-range tails lifts the classical degeneracy in the fully packed dimer coverings subspace [30]. This fact generates a complex pattern of phases between the maximal-density components of the prepared state, yielding suppressed overlaps between the RVB state and the state reached at the end of the sweep in Fig. 1(a). We refer to [26] for a more detailed discussion of this issue, and we stress here that high RVB fidelities are obtained when only the absolute value of the components of the prepared state is considered. Gaining a deeper understanding of the effect of these phases and their control is crucial for the experimental applicability of the preparation protocol discussed in the first part of this Letter.

We now focus on the ansatz Eq. (2) and compare it to the state dynamically prepared at finite Δ/Ω. We note that the constraint relaxation produces a non-negligible projection of the latter on the subspace violating the dimer constraint [10]. In an attempt to capture this constraint-violating component, we remove the projector $\mathcal{P}$ in the overlap optimization. The resulting state-phase diagram is qualitatively unchanged with respect to the one in Fig. 3 [26]. We plot in Fig. 4(a) the outcome of the optimization for a periodic cluster of $N = 36$ atoms, for various total sweep times T (solid lines), and including the fully adiabatic sweep (dashed line). The result is analogous to the one depicted in Fig. 2(a) for the PXP model, where the smaller maximal overlaps are to be compared with the much larger Hilbert space dimension: 2^{24} vs $\simeq 2^{17}$ for $N = 36$. Remarkably, the fidelity per site increases with increasing N for the two system sizes considered [Fig. 4(b)].

Outlook.—We discussed dynamical preparation of topological spin liquids in Rydberg atom arrays. First, we showed that the pure RVB state can be reached with impressively high fidelity in a time that scales linearly with the number of atoms. Although the optimal preparation times needed to reach the highest fidelities are somewhat longer than those accessible in the current experimental capabilities [31], further optimization, larger Rabi frequencies, as well as improved coherence in experiments could make defect-free RVB state preparation feasible. We also showed that the nonequilibrium state observed in [10] is well described by a two-parameter family of TN states with small bond dimension. The latter includes the topologically ordered RVB state and the vacuum. We exploit this TN representation to study the properties of the prepared state on unprecedentedly large

systems, and infer about the stability of topological order in the thermodynamic limit. We find that our ansatz is fully consistent with a topological spin liquid in a finite region in parameter space. Our Letter clarifies the nature of nonequilibrium state experimentally prepared in [10], and provides the tools for performing large-scale classical simulations that might serve as guidance for probing topological quantum matter in future quantum simulator experiments. These studies can be extended along several directions. For instance, our approach can be used to explore nontrivial dynamics of anyonic excitations as well as the preparation of the other topologically degenerate states that have a natural interpretation within the TN framework [32]. Moreover, the dynamical preparation of the pure RVB state is not limited to the ruby lattice described in the present Letter. In particular, one can explore if this method can be applied to other systems with a ground state degeneracy growing exponentially with the number of atoms (see, e.g., Ref. [33]). In such systems dynamical preparation protocols can be potentially used to engineer other kinds of exotic phases of matter in a wide variety of lattice geometries.

We acknowledge useful discussions with I. Cong, G. Giudice, N. Maskara, S. Sachdev, R. Samajdar, G. Semeghini, R. Verresen, A. Vishwanath, and T. Zache. This research was supported by the Army Research Office (Grant No. W911NF-21-1-0367), the ERC Starting Grant QARA (Grant No. 101041435), a discovery grant by the Erwin Schrödinger Center for Quantum Science, CUA, NSF, and DOE. G. G. acknowledges support from the Deutsche Forschungsgemeinschaft (DFG, German Research Foundation) under Germany's Excellence Strategy–EXC-2111–390814868 and from the ERC grant QSIMCORR, ERC-2018-COG, No. 771891.

Note added.—Recently, we became aware of a related variational study of nonequilibrium topological state preparation, Ref. [34].

[1] N. Read and S. Sachdev, Phys. Rev. Lett. **66**, 1773 (1991).
[2] X. G. Wen, Phys. Rev. B **44**, 2664 (1991).
[3] S. Sachdev, Phys. Rev. B **45**, 12377 (1992).
[4] L. Savary and L. Balents, Rep. Prog. Phys. **80**, 016502 (2017).
[5] X.-G. Wen, Rev. Mod. Phys. **89**, 041004 (2017).
[6] S. Sachdev, Rep. Prog. Phys. **82**, 014001 (2019).
[7] A. Y. Kitaev, Ann. Phys. (Amsterdam) **303**, 2 (2003).
[8] F. Wilczek, Phys. Rev. Lett. **49**, 957 (1982).
[9] C. Nayak, S. H. Simon, A. Stern, M. Freedman, and S. Das Sarma, Rev. Mod. Phys. **80**, 1083 (2008).
[10] G. Semeghini, H. Levine, A. Keesling, S. Ebadi, T. T. Wang, D. Bluvstein, R. Verresen, H. Pichler, M. Kalinowski, R. Samajdar, A. Omran, S. Sachdev, A. Vishwanath, M. Greiner, V. Vuletić, and M. D. Lukin, Science **374**, 1242 (2021).
[11] R. Verresen, M. D. Lukin, and A. Vishwanath, Phys. Rev. X **11**, 031005 (2021).
[12] D. Jaksch, J. I. Cirac, P. Zoller, S. L. Rolston, R. Côté, and M. D. Lukin, Phys. Rev. Lett. **85**, 2208 (2000).
[13] M. D. Lukin, M. Fleischhauer, R. Cote, L. M. Duan, D. Jaksch, J. I. Cirac, and P. Zoller, Phys. Rev. Lett. **87**, 037901 (2001).
[14] E. Urban, T. A. Johnson, T. Henage, L. Isenhower, D. D. Yavuz, T. G. Walker, and M. Saffman, Nat. Phys. **5**, 110 (2009).
[15] A. Gaëtan, Y. Miroshnychenko, T. Wilk, A. Chotia, M. Viteau, D. Comparat, P. Pillet, A. Browaeys, and P. Grangier, Nat. Phys. **5**, 115 (2009).
[16] D. S. Rokhsar and S. A. Kivelson, Phys. Rev. Lett. **61**, 2376 (1988).
[17] R. Moessner and S. L. Sondhi, Phys. Rev. Lett. **86**, 1881 (2001).
[18] R. Moessner and K. S. Raman, *Introduction to Frustrated Magnetism*, edited by C. Lacroix, P. Mendels, and F. Mila, Springer Series in Solid-State Sciences Vol. 164 (Springer, Berlin, Heidelberg, 2011).
[19] P. W. Anderson, Mater. Res. Bull. **8**, 153 (1973).
[20] J. Bricmont and J. Frölich, Phys. Lett. **122B**, 73 (1983).
[21] K. Fredenhagen and M. Marcu, Commun. Math. Phys. **92**, 81 (1983).
[22] A. Kitaev and J. Preskill, Phys. Rev. Lett. **96**, 110404 (2006).
[23] M. Levin and X.-G. Wen, Phys. Rev. Lett. **96**, 110405 (2006).
[24] M. Saffman, T. G. Walker, and K. Mølmer, Rev. Mod. Phys. **82**, 2313 (2010).
[25] A. Browaeys and T. Lahaye, Nat. Phys. **16**, 132 (2020).
[26] See Supplemental Material at http://link.aps.org/supplemental/10.1103/PhysRevLett.129.090401, which includes Ref. [27] for an introduction on transfer matrices of tensor network states.
[27] V. Zauner, D. Draxler, L. Vanderstraeten, M. Degroote, J. Haegeman, M. M. Rams, V. Stojevic, N. Schuch, and F. Verstraete, New J. Phys. **17**, 053002 (2015).
[28] S. Ji, C. Ates, and I. Lesanovsky, Phys. Rev. Lett. **107**, 060406 (2011).
[29] The range of Δ/Ω where the maximum optimized overlaps are obtained do not depend on N for fixed T, as long as the latter is chosen proportional to N.
[30] Interestingly, the fully packed dimer configurations remain exactly degenerate upon inclusion of the shortest interaction beyond the blockade.
[31] Maximum RVB overlaps are obtained for a total preparation time $\Omega T \simeq 4.5N$. While the preparation time in the experiments [10] was shorter than this predicted optimal time, the experiments utilized optimized, nonlinear detuning sweeps to create QSL states with reduced defect density.
[32] N. Schuch, I. Cirac, and D. Pérez-García, Ann. Phys. (Amsterdam) **325**, 2153 (2010).
[33] R. Samajdar, W. W. Ho, H. Pichler, M. D. Lukin, and S. Sachdev, Proc. Natl. Acad. Sci. U.S.A. **118** (2021).
[34] Y. Cheng, C. Li, and H. Zhai, arXiv:2112.13688.